Cytochrome *c* and Organic Molecules: Solution Structure of the *p*-Aminophenol Adduct[†,‡]

Michael Assfalg,[§] Ivano Bertini,*[,§,||,⊥] Rebecca Del Conte,[§] Andrea Giachetti,[§,||,@] and Paola Turano[||,⊥]

ProtEra srl, viale delle idee 22, 50019 Sesto Fiorentino, Italy, Magnetic Resonance Center (CERM), University of Florence, Via Luigi Sacconi 6, 50019 Sesto Fiorentino, Italy, Department of Chemistry, University of Florence, Via della Lastruccia 3, 50019 Sesto Fiorentino, Italy, and Department of Agricultural Biotechnology, University of Florence, Piazzale delle Cascine 24, 50144 Firenze, Italy

Received February 9, 2007; Revised Manuscript Received March 27, 2007

ABSTRACT: Protein−protein interactions are driven by specific properties of the molecular surfaces. Cytochrome *c*, a small electron transfer protein, is involved in a number of biologically relevant interactions with macromolecular partners. Small molecules may interfere with such interactions by binding to the surface of cytochrome *c*. Here we investigated the possibility of weak intermolecular interactions between reduced cytochrome *c* and a library of 325 small molecules, using WaterLOGSY NMR spectroscopy. Specific binding was found for *p*-aminophenol. The solution structure of the *p*-aminophenol−cytochrome *c* adduct was determined using a combination of in silico tools and NMR-based restraints. The ligand interacts in a specific binding site on the protein surface through a combination of stacking and H-bond interactions. Small but meaningful rearrangements of the solvent-exposed side chains are observed upon ligand binding and contribute to the stabilization of the complex.

The field of drug discovery is dominated by screening small molecules toward enzymes as pharmaceutical targets. Among the various strategies, a combination of in silico tools and NMR analysis represents a fruitful approach for the fast obtainment of structural models highlighting the key interactions of ligands in the enzymatic cavity and for guiding a cyclic procedure for optimization of drug candidates (*1*−*4*). However, the discovery of an increasing number of functional interactions among proteins is moving the focus of drug design toward the characterization of the binding properties of protein surfaces. Therefore, the number of pharmaceutically relevant targets increases and extends to proteins that do not contain specific cavities or binding sites for ligand molecules. Protein surfaces frequently contain hot spots (*5*), i.e., small patches that are the main mediators of binding affinity. The idea of targeting these protein areas is gaining new attention after the recent identification of small-molecule inhibitors of several protein−protein systems in the oncology area, culminating with the discovery of selective druglike inhibitors of the murine double minute-2−proto-oncogene (MDM2−p53) interaction (*6*).

[†] This work was supported by PRIN-2005 from the Ministero Italiano dell'Università e della Ricerca (MIUR), by Fondazione Monte dei Paschi di Siena 2005, and by EC contracts: Marie Curie-TOK Contract MTKI-CT-2004-509750, NDDP contract LSHG-CT-2004-512077, and Nano4Drugs contract LSHB-CT-2005-019102.

[‡] The Protein Data Bank entries are 2HV4 (unbound cytochrome *c*) and 2ORL (adduct).

* To whom correspondence should be addressed: Magnetic Resonance Center (CERM), University of Florence, Via Luigi Sacconi, 6, 50019 Sesto Fiorentino (Florence), Italy. Phone: +39 0554574270. Fax: +39 0554574273. E-mail: ivanobertini@cerm.unifi.it.

[§] ProtEra srl.

[||] Magnetic Resonance Center (CERM), University of Florence.

[⊥] Department of Chemistry, University of Florence.

[@] Department of Agricultural Biotechnology, University of Florence.

We present here a study of the binding properties of the mitochondrial yeast cytochrome *c* surface toward a number of small organic molecules. Cytochrome *c* is a small electron transfer protein (108 amino acids) (*7*). The protein fold is characterized by the presence of five α-helices and fairly extended loop structures. The covalently bound heme prosthetic group is buried within a hydrophobic pocket. The heme iron coordination is completed by a His and a Met as axial ligands: the proximal His18 belongs to the consensus sequence Cys-X-Y-Cys-His, with the two Cys residues being involved in the thioether bonds that provide the covalent linkage of the heme to the protein chain; the axial Met80 belongs to a relatively long loop preceding the long C-terminal helix. The Met80 bond is relatively labile and may be easily replaced by exogenous ligands (*8*−*13*). The protein is highly basic, with several surface lysines that impart anion binding properties to the cytochrome *c* surface (*14*−*17*). The binding ability of a number of potential organic ligands was here tested, and the structure of the adduct with the best behaving ligand was calculated. As the oxidized iron(III) form of the protein has a strong tendency to autoreduce during NMR measurements (*18*), the reduced diamagnetic iron(II) form was used in this study. The determination of the structure of the protein−ligand adduct was achieved through an implemented protocol (*3*) that allows the quick determination of the binding mode of small molecules on the protein surface through a NMR-assisted in silico approach. The results underline the potentiality of the NMR approach to characterizing weak interactions between proteins and their ligands.

EXPERIMENTAL PROCEDURES

Sample Preparation. Unlabeled, ^{15}N-enriched, and ^{15}N- and ^{13}C-doubly labeled yeast iso-1-cytochrome *c* was

10.1021/bi7002857 CCC: $37.00
Published on Web 05/09/2007

expressed and purified as previously described (*18*). The reduced protein was obtained by adding 2 equiv of sodium dithionite under anaerobic conditions. Ligand molecules for WaterLOGSY[1] experiments were added from stock solutions in dimethylsulfoxide (DMSO) of a library of molecules (4 μL of stock solution in a total volume of 500 μL, to provide a final concentration of 0.8 mM in ligand). For further characterization, ligand molecules were added directly as a solid, to avoid chemical shift differences in protein resonances induced by the presence of DMSO. The protein concentration in WaterLOGSY experiments was 8 μM. For ^{1}H$-^{15}$N HSQC experiments, the protein concentration was on the order of 60 μM. The three-dimensional (3D) ^{15}N HSQC-NOESY spectrum was acquired on a 1 mM protein sample, with a protein:*p*-aminophenol molar ratio of 1:6. All the samples were in 50 mM phosphate buffer at pH 7.

NMR Experiments. NMR spectra were recorded at 303 K. For the interaction studies, WaterLOGSY (*19*) experiments were conducted on a Bruker AVANCE 700 MHz spectrometer equipped with a 5 mm triple-resonance TXI, Z-gradient probe, and an automatic sample changer. WaterLOGSY NMR experiments employed a 2 ms selective rectangular 180° pulse at the water signal frequency and a NOE mixing time of 2 s. ^{1}H$-^{15}$N HSQC (*20*) and 3D ^{15}N NOESY-HSQC (*21*) (mixing time of 100 ms) experiments were conducted on Bruker AVANCE 900 and 800 MHz spectrometers, both equipped with a cryoprobe. The acquisition parameters for these NMR spectra are provided as Supporting Information (Table S1).

For the assignment of backbone and side chain resonances of the free protein sample, the following experiments were conducted at 800 MHz, in the same buffer conditions specified above for the 3D NOESY spectrum: HNCA, HN(CO)CA, CBCA(CO)NH, H(C)CH-TOCSY, and CCC(CO)NH. An HNHA experiment was performed at 700 MHz to obtain dihedral angle restraints, and a 3D ^{15}N NOESY-HSQC (mixing time of 100 ms) experiment was conducted to obtain distance restraints.

Structure Calculations and Refinement. Assignment of NOESY cross-peaks was performed with the aid of CORMA which predicts NOEs expected for a given structure (*22*). Distance restraints for structure determination of the free protein were obtained from 3D ^{15}N NOESY-HSQC experiments and from two-dimensional (2D) NOESY, by converting NOE cross-peak intensities into upper distance limits of interproton distances with CALIBA (*23*). $^3J_{\mathrm{HNH}\alpha}$ coupling constants were determined from the HNHA experiment (*24*) and transformed into backbone dihedral ϕ angles via the Karplus equation. Backbone dihedral ψ angles for residue $i - 1$ were also determined from the ratio of the intensities of the $\mathrm{H}\alpha_{i-1}-\mathrm{HN}_i$ and $\mathrm{H}\alpha_i-\mathrm{HN}_i$ NOEs found on the ^{15}N plane of residue i in the 3D ^{15}N NOESY-HSQC spectrum (*25*). Residual dipolar couplings (RDC) restraints were previously obtained from measurements of amide ^{15}N$-^1$H ^1J couplings at 800 and 500 MHz and were introduced into the structure calculations as reported previously (*26*). The relative weights of all restraints were taken to be equal to 1, and the tolerance values (T_i) for the RDC were taken to be equal to the estimated experimental errors. A family of structures was generated starting from random conformations with an implementation of DYANA (*27*) (information on program available at www.postgenomicnmr.net). The heme cofactor was introduced into the structure calculations as described previously (*28*). The coordination bond between the iron ion and the axial ligands was introduced using upper and lower distance limits between the iron and the donor atoms. The molecular magnetic susceptibility tensor for the diamagnetic iron(II) protein was treated as described elsewhere (*26*), using the tensor values reported previously (*26*). Five hundred random structures were annealed in 10 000 steps under the effect of NMR restraints. The final family of structures with the lowest target function was energy-minimized with AMBER 8.0 (*29*), imposing the same set of experimental restraints used in DYANA. The NOE and torsion angle restraints were applied with force constants of 50 kcal mol^{-1} Å^{-2} and 32 kcal mol^{-1} rad^{-2}, respectively.

Table 1: Main Features of the Molecules Constituting the Screened Library of Compounds

descriptor	minimum value	maximum value
molecular weight	68.07	776.87
no. of atoms	8	80
no. of rings	0	6
ring size (no. of atoms)	3	7[a]
LogP[b]	−2.48	8.8
ClogP[c]	−9.20	9.32
no. of H-bond donors	0	5[d]
no. of H-bond acceptors	0	6

[a] A single compound has a ring size of 12. [b] Logarithm of the partition coefficient between *n*-octanol and water. [c] Logarithm of the octanol:water partition coefficient (LogP) computed using the semiempirical fragment-based method. [d] A single compound contains eight H-bond donors.

The structure calculations of the cytochrome *c*$-$*p*-aminophenol complex were performed using a combination of Autodock and XPLOR-NIH (*3*). Initial protein$-$ligand adducts were generated by running a lamarckian genetic algorithm docking with Autodock. The search grids were centered around the protein residues that exhibited significant chemical shift perturbations upon ligand addition and were constituted by 70 × 70 × 70 grid points with a spacing of 0.253 Å. One hundred runs were allowed for each calculation. The resulting structures were clustered according to Autodock energy. The lowest-energy structures were used as input for a subsequent refinement procedure using XPLOR-NIH in the presence of distance restraints derived from the 906 intraprotein and the four intermolecular NOEs obtained from the 3D ^{15}N NOESY-HSQC spectrum of the adduct, as well as using 39 angle restraints based on the $\mathrm{H}\alpha_{i-1}-\mathrm{HN}_i/\mathrm{H}\alpha_i-\mathrm{HN}_i$ NOE ratios. Intermolecular connectivities were all converted into upper distance limits of 6 Å. Intraprotein connectivities were translated into upper distance limits using CALIBA (*23*). The resulting structures were ordered according to a target function calculated considering the ligand$-$residue and residue$-$residue interactions.

RESULTS AND DISCUSSION

Identification of Cytochrome c Ligands. A now well-established approach for NMR-based drug screening of large libraries of compounds is based on the so-called WaterLOGSY experiments (*19*). The WaterLOGSY (water$-$ligand

[1] Abbreviations: CSP, chemical shift perturbation; HSQC, heteronuclear single-quantum coherence; NOESY, nuclear Overhauser effect spectroscopy; PAF, *p*-aminophenol; WaterLOGSY, water ligand observed via gradient spectroscopy; RDC, residual dipolar couplings.

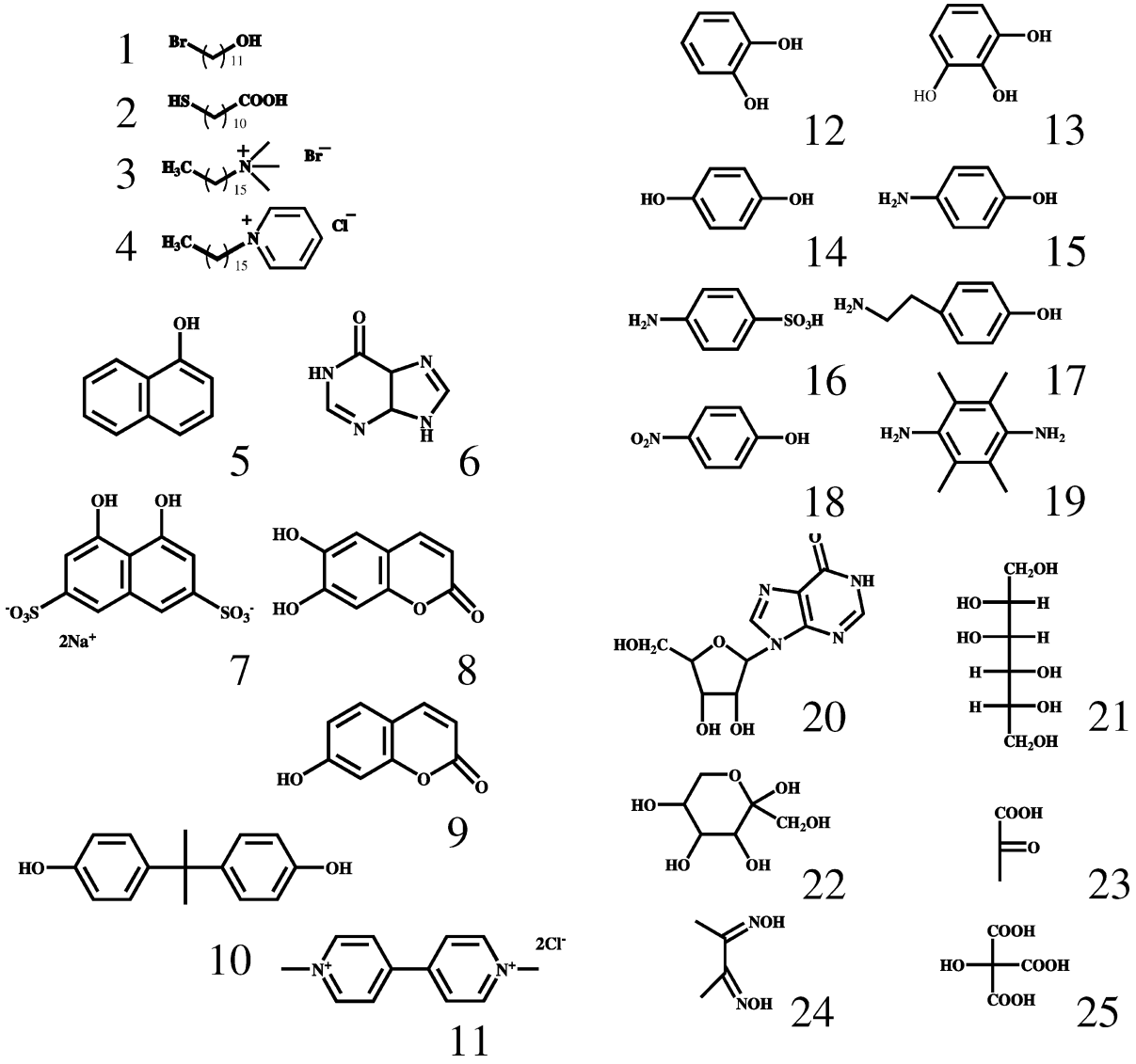

FIGURE 1: Chemical structures of molecules for which a change in sign or significant signal reduction in intensity in the WaterLOGSY experiments recorded in the presence of the protein was observed.

observed via gradient spectroscopy) technique relies on excitation of the receptor−ligand complex through a selective radiofrequency pulse scheme that is achieved indirectly by selective perturbation of the bulk water magnetization. Distinguishing binding from nonbinding compounds in the WaterLOGSY experiment is achieved by observing the differential cross-relaxation properties of these ligands with water. The bound ligands interact directly or indirectly with inverted water spins via dipolar interactions with sufficiently long rotational correlation times (τ_c) to yield negative cross-relaxation rates. By contrast, the dipolar interactions of nonbinders with water have much shorter τ_c values, leading to positive cross-relaxation rates. As a consequence, WaterLOGSY peak intensities provide an easy means of discriminating between binders and nonbinders. This method allows screening of large libraries of compounds using relatively small amounts of unlabeled receptor. The analysis of the possible interactions involving cytochrome *c* and potential ligand molecules was performed by a NMR screening against a library of 325 compounds. The main features of the library of molecules are reported in Table 1. For 25 molecules, listed in Figure 1, WaterLOGSY experiments indicated binding to cytochrome *c*.

The interaction mode of each of these 25 molecules with cytochrome *c* was further investigated using the chemical shift perturbation (CSP) mapping approach. As opposed to the WaterLOGSY experiment which can be described as a ligand-observe method, CSP mapping is based on observation of the protein signals. Generally, a ^{15}N-labeled receptor is analyzed in the presence of unlabeled ligands using heteronuclear correlation spectroscopy experiments, such as ^{1}H−^{15}N HSQC. Because chemical shifts are very sensitive indicators of the local electronic environment of the nuclei, monitoring their perturbations provides a straightforward means of detecting binding events as well as of determining the involved amino acid residues, once the cross-peak assignments are available. Having reduced the number of potential binders from the compound library by WaterLOGSY screening, we were then able to use the more costly ^{15}N-labeled protein for CSP mapping. The experiments were conducted in the presence of an excess of the ligand molecule, with the aim of identifying specific binding sites on the protein surface. It appears that bulky ligands like 4,4′-isopropylidenediphenol and 1,1-dimethyl-4,4′-bipyridinium dichloride (Figure 1, compounds **10** and **11**, respectively) are aspecifically interacting and induce chemical shift

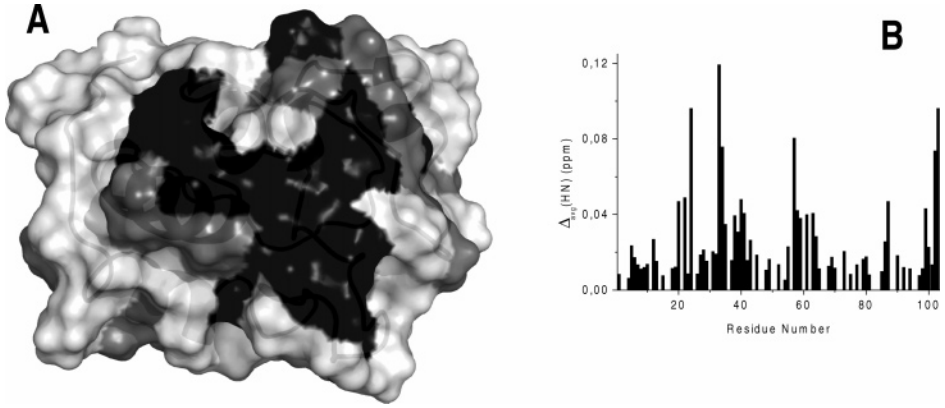

FIGURE 2: (A) Cytochrome *c* surface residues experiencing chemical shift differences upon binding of aromatic molecules with H-bond donor and/or acceptor substituents. Residues highlighted in gray experience CSPs in the range of 0.01−0.04 ppm. Residues highlighted in black experience CSPs larger than 0.04 ppm. (B) Plot of the observed CSP, extrapolated to 100% bound, as a function of the residue number.

changes on a very limited number of resonances scattered in different protein areas. Condensed and conjugated aromatic compounds (Figure 1, compounds **5**−**9**) have a similar behavior. Polyalcohols and sugars (Figure 1, compounds **20**−**25**) also exhibit weak aspecific interactions. Long chain aliphatic molecules (Figure 1, compounds **1**−**4**) with a polar term interact with surface residues of cytochrome *c*. While SDS induces protein unfolding (*30*), other long chain molecules do not alter the protein structure. The presence of bulky polar edges causes a loss of affinity and specificity (this is the case for molecule **4**). Binding of 11-bromo-1-undecanol induces heme iron oxidation. Nevertheless, in the presence of all the molecules mentioned above, the observed combined $^1H-^{15}N$ shift perturbation upon complexation (given by $\Delta_{av} = \{[\Delta\delta_{HN}^2 + (\Delta\delta_N/5)^2]/2\}^{1/2}$) (*31*) for cytochrome *c* backbone amides is always smaller than 0.04 ppm, suggesting a weak dynamic binding (*2*, *32*) that is rather scattered on the protein surface (Figure S1 of the Supporting Information), suggesting a lack of specificity.

On the other hand, monoaromatic molecules with H-bond donor and/or acceptor substituents (Figure 1, compounds **12**−**19**) are found to bind specifically in the same protein area, giving rise to chemical shift differences as large as 0.13 ppm. These molecules all induce chemical shift changes on a few selected residues on the protein surface. For all of them, fast exchange between the bound and unbound protein resonances was observed. The relative affinity within this series of compounds is modulated by the nature and relative position of the ring substituents. Para-substituted compounds are invariably better than the corresponding ortho and meta derivatives. Among the para derivatives, the largest effect is obtained with *p*-aminophenol (see Figure 2). The distance between the amino and hydroxyl groups appears to be critical for the interaction, the chemical shift changes being smaller in the case of tyramine (compound **17** in Figure 1).

From the chemical shift deviations observed upon complex formation (*2*) and from WaterLOGSY experiments (*19*) with different amounts of inhibitor, a rough estimate of K_d in the range 50−100 μM for the binding of *p*-aminophenol to cytochrome *c* was obtained. Given its higher specificity, the *p*-aminophenol was selected for investigation of the nature of the interactions leading to the formation of the adduct. 3D ^{15}N NOESY-HSQC experiments were conducted with cytochrome *c* in the presence and absence of the ligand

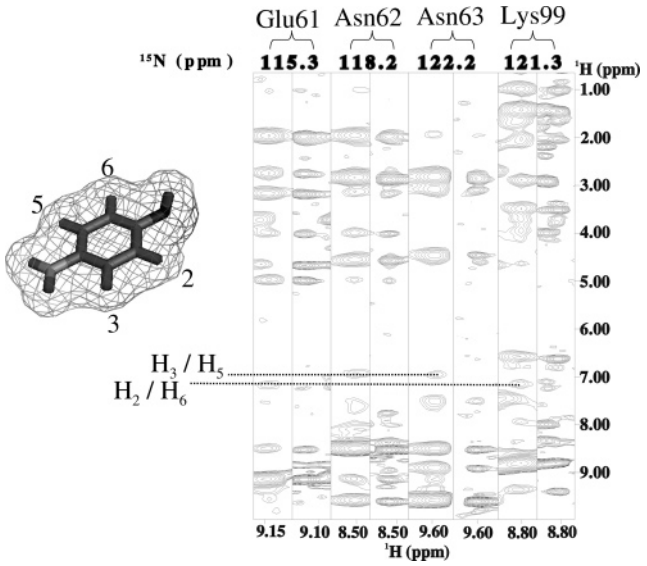

FIGURE 3: 3D ^{15}N NOESY-HSQC strips for the four protein amino acids showing NOEs with respect to the ligand molecule. For each amino acid, the first strip represents the NOESY spectrum in the presence of the ligand and the second strip the corresponding spectrum recorded in the absence of the ligand molecule.

molecule. This spectrum allowed the detection of four NOEs between ligand protons and protein protons. The latter are the backbone amides of residues Glu61, Asn62, and Asn63 on the 60S helix and Lys99 on the C-terminal helix. As depicted in Figure 3, the cross-peaks for the observed intermolecular NOEs (Glu61 H_N−PAF $H_{2,6}$, Lys99 H_N−PAF $H_{2,6}$, Asn62 H_N−PAF $H_{3,5}$, and Asn63 H_N−PAF $H_{3,5}$) were absent in the free protein spectrum and not attributable to nuclei of other neighboring protein residues.

As verified by monodimensional ^1H NMR experiments, the heme iron coordination was not affected by the presence of the exogenous ligand.

Refinement of the Solution Structure of Unbound Yeast Cytochrome c. In the case of reduced yeast cytochrome *c*, both X-ray and NMR solution structures are available (*33*, *34*). Deciphering the surface properties of cytochrome *c* requires a high-resolution structure. To avoid biases on protein conformation due to crystal packing effects, we decided to start from the NMR solution structures of the target protein. The NMR structure of reduced yeast cytochrome *c* had been determined many years ago by some of

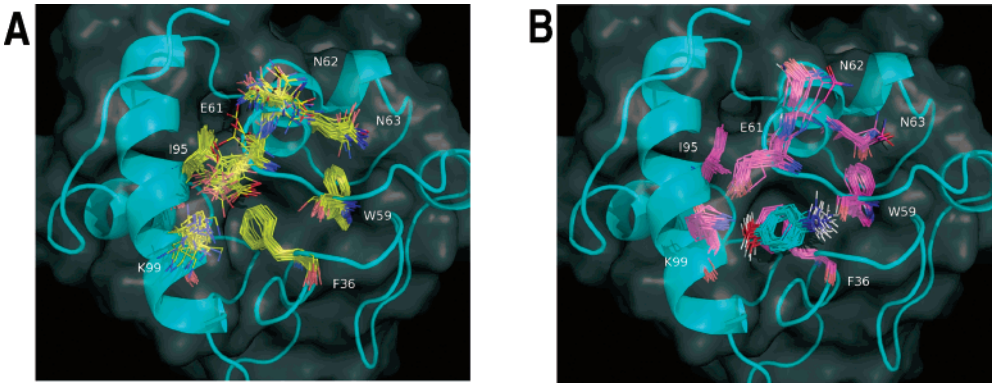

FIGURE 4: Binding site of *p*-aminophenol. The families of structures of unbound (A) and bound (B) cytochrome *c* are shown to highlight the different orientation of Lys99 and Glu61. The Phe36 ring is also displayed to show the stacking interaction between its aromatic ring and that of the ligand molecule in the adduct.

us using ^{1}H-only NMR experiments (*34*). Prior to the obtaining the solution structure of the adduct, we refined the solution structure of cytochrome *c* here, with the use of ^{1}H−^{15}N-based NMR experiments that provide an increased spectral resolution and the use of a larger set of experimental restraints. Indeed, we have increased the number of meaningful NOEs; there are now 1686, compared to 1442 of the previous structure. We have added a total of 108 dihedral ϕ and ψ angle restraints derived from HNHA (*24*) and from the ratio between sequential and intraresidue Hα−HN cross-peaks in 3D NOESY NMR experiments (*25*), and we have made use of residual dipolar coupling restraints due to self-orientation of the diamagnetic protein (*26*). The resulting family of structures is larger (35 members vs 20 members of the original family of structures with a target function lower than 0.82 Å^2) and more precise, with backbone rmsd values and all heavy atom rmsd values with respect to the mean for residues −1 to 102 of 0.54 ± 0.08 and 0.99 ± 0.08 Å, respectively. The previous family of 20 structures (PDB entry 1YFC) (*34*) had backbone rmsd and all heavy atom rmsd values with respect to the mean of 0.61 ± 0.09 and 0.98 ± 0.09 Å, respectively, considering only residues 6−100. The analysis of the quality for this structure is provided as Supporting Information (Table S2), and the coordinates have been deposited in the Protein Data Bank (entry 2HV4). The use of a larger set of experimental restraints as well as restraints of a different nature made us more confident in the obtained structural data.

Solution Structure of the Adduct. The structure calculations for the adduct were performed using Xplor-NIH (*35*). As a starting protein structure, the best one (in terms of agreement with experimental restraints) of the family of structures of unbound cytochrome *c* determined as described above was taken. The ^{1}H−^{15}N HSQC-determined chemical shift variations upon ligand binding were used to define the grid for in silico docking with Autodock. The lowest-energy structures from Autodock were used for the subsequent Xplor-NIH complex structure calculations (*3*). The four experimental intermolecular NOEs and the 906 intramolecular NOEs derived from 3D ^{15}N NOESY-HSQC experiments were translated into upper distance limits and used as experimental restraints together with 39 NOE-derived angle restraints. This approach is a modification of that proposed by some of us (*3*), where only the interresidue NOEs were used as experimental restraints and the backbone atoms of residues experiencing chemical shift differences in ^{1}H−^{15}N HSQC experiments and all the protein side chains were left free to move, thus allowing a better docking with respect to programs where the protein is completely rigid. Here we employ as experimental restraints the whole set of upper distance limits derived from 3D ^{15}N NOESY-HSQC NOEs (both inter- and intraresidue), and the whole protein is left free to move. Using a complete set of experimental constraints for all protein residues made us confident that all the observed conformational changes are experimentally supported and that the mapping of possible residues involved in the interaction is not limited only to those experiencing chemical shift variations for their backbone amides in ^{1}H−^{15}N HSQC experiments.

A final family of 25 structures characterized by the lowest energy values was selected (PDB entry 2ORL), and the member of the family with the lowest total energy is reported in Figure 4. In all these structures, the *p*-aminophenol ring and the aromatic ring of Phe36 interact in an offset or slipped stacking (*36*−*39*). The average distance between the aromatic ring centers is on the order of 4.5 Å, and the two planes are invariably parallel to one another in all the structures of the family (average angle between the two planes of 9 ± 4°), with an average distance between them of 3.4 ± 0.1 Å. The parallel displacement therefore corresponds to ∼2.9 Å. The other major intermolecular interaction involves the OH group on the ligand molecule, which gives rise to a H-bond with the side chain of Lys99, with O−N distances on the order of 2.8 Å. The latter residue sensibly changes its orientation with respect to the unbound cytochrome. In general, the rmsd values for the backbone and heavy atoms between the average structures of unbound and bound cytochrome *c* are 0.49 ± 0.21 and 0.84 ± 0.36 Å, respectively. These deviations are much larger for the heavy atoms of Lys99, being on average 2.2 Å. This finding is strongly supported by our experimental observation that Lys99 is the residue that experiences the largest changes in chemical shift for the side chain protons and has the largest changes in intra- and interresidue NOE intensities upon ligand binding. The Lys99 side chain is further stabilized in its new orientation through the interaction with the side chain of Glu61 (with N−O1 and N−O2 distances on the order of 2.7 and 2.9 Å, respectively), which also shows a conformational change with respect to unbound cytochrome *c*.

The residues involved in the interaction (i.e., Phe36, Lys99, and Glu61) are all well-defined, with rmsd values for the side chain heavy atoms of 0.34, 0.40, and 0.43 Å, respec-

tively. The heavy atom rmsd for the ligand molecule is 0.44 Å. Our spectra show that the interaction with Phe36 does not appreciably slow the flip rate of its aromatic ring.

CONCLUSIONS

Cytochrome *c* is a small, globular, and soluble protein. For this reason, it has been the subject of many structural studies in solution by NMR. Most of these studies aimed to characterize the protein conformation in the two functional redox states, iron(III) and iron(II) (*18*, *28*, *34*, *40*−*42*), even in the presence of exogenous ligands substituting the native Met80 in the sixth coordination position of the heme iron (*8*, *9*, *43*−*47*). Typical small molecules able to enter the distal site of the heme are CN^-, NH_3, and imidazole, i.e., molecules with a high affinity for the distal site of the protein. The determination of the structure of the protein in the presence of such molecules has provided important insight into the role of some amino acid side chains in the distal site of the protein for stabilizing such ligands as well as into the electronic structure and structural stability of the protein. A number of other studies aimed to identify anion binding sites on the protein surface (*14*−*17*). To the best of our knowledge, our study represents the first determination of the structure of cytochrome *c* bound to a non-heme binding non-anionic ligand.

These results underline how the combination of NMR and in silico investigations allows the determination at atomic resolution of the mode of binding of small molecules to the surface of proteins lacking any deep pocket. Chemical shift mapping had a fundamental role in defining the surface area to be investigated by the docking procedure. Few but well-defined intermolecular NOEs represented the key restraints for the definition of the position of the *p*-aminophenol on the protein surface and for the correct filtering of the docking solutions.

We tried initially to identify cavities and clefts with the use of standard software for surface analysis (*48*), but no such features were found on the cytochrome *c* surface. Still, the chemical properties of certain amino acids on the protein surface are able to create a site that can properly interact with the *p*-aminophenol molecule. Analogous adaptive spots on protein surfaces undergoing reorientation of protein side chains upon binding of a small molecule have been reported by other authors (*49*, *50*). In particular, the adaptive spot on the cytochrome *c* surface identified here seems to be capable of supporting binding of ligands thanks to a combination of effects: the presence of an exposed aromatic residue, Phe36, that may give rise to stacking interactions with the aromatic ring of the ligand and polar side chains that could reorient upon binding to optimize H-bonds with the amino and phenol groups on the ligand molecule. The stacking interaction appears to be the key factor for the binding of any of the monoaromatic species in Figure 1. However, the presence of selected side chains (Lys99 and Glu61) of the protein at given distances makes the *p*-aminophenol the best ligand. Long chain aliphatic molecules with a polar terminus were also found to interact with cytochrome *c* surface residues, although with an affinity and specificity lower than those of *p*-aminophenol. From the chemical shift perturbation plot, the binding site appears to be distinct from that of monoaromatic species. Long chain molecules could be considered in a later development of the project, aimed at fragment-based design of high-affinity ligands for the cytochrome *c* surface (*51*, *52*). Indeed, during the past decade, mitochondrial cytochrome *c* has emerged as a one of the key players in cellular apoptosis (*53*) in multicellular organisms. Mapping of its surface binding properties is therefore relevant for the inhibition of anti- and pro-apoptotic intermolecular interactions. Although these experiments were conducted on the yeast protein, the results are also relevant for the mammalian and, in particular, human cytochrome *c*. Indeed, in all these proteins, the key residues for the interaction with *p*-aminophenol (i.e., Phe36, Glu61, and Lys99) are conserved (*54*).

SUPPORTING INFORMATION AVAILABLE

Acquisition parameters for the NMR experiments, statistical analysis of the solution structure of unbound *Saccharomyces cerevisiae* iso-1-cytochrome *c*, the number of intramoleuclar NOEs involving side chains in the binding site of PAF, and CSP for some of the screened molecules. This material is available free of charge via the Internet at http://pubs.acs.org.

REFERENCES

1. Homans, S. W. (2004) NMR spectroscopy tools for structure-aided drug design, *Angew. Chem., Int. Ed. 43*, 290−300.
2. Meyer, B., and Peters, T. (2003) NMR spectroscopy techniques for screening and identifying ligand binding to protein receptors, *Angew. Chem., Int. Ed. 42*, 864−890.
3. Bertini, I., Fragai, M., Giachetti, A., Luchinat, C., Maletta, M., Parigi, G., and Yeo, K. J. (2005) Combining in silico tools and NMR data to validate protein-ligand structural models: Application to matrix metalloproteinases, *J. Med. Chem. 48*, 7544−7559.
4. Constantine, K. L., Davis, M. E., Metzler, W. J., Mueller, L., and Claus, B. L. (2006) Protein-ligand NOE matching: A high-throughput method for binding pose evaluation that does not require protein NMR resonance assignments, *J. Am. Chem. Soc. 128*, 7252−7263.
5. Trosset, J.-Y., Dalvit, C., Knapp, S., Fasolini, M., Veronesi, M., Mantegani, S., Gianellini, L. M., Catana, C., Sundstrom, M., Stouten, P. F., and Moll, J. K. (2006) Inhibition of protein-protein interactions: The discovery of druglike β-catenin inhibitors by combining virtual and biophysical screening, *Proteins 64*, 60−67.
6. Vassilev, L., Vu, B., Graves, B., Carvajal, D., Podlaski, F., Filipovic, Z., Kong, N., Kammlott, U., Lukacs, C., Klein, C., Fotouhi, N., and Liu, E. A. (2004) In vivo activation of the p53 pathway by small-molecule antagonists of MDM2, *Science 303*, 844−848.
7. Scott, R. A. and Mauk, A. G. (1996) *Cytochrome c. A multidisciplinary approach*, University Science Books, Sausalito, CA.
8. Banci, L., Bertini, I., Liu, G., Reddig, T., Tang, W., Wu, Y., and Zhu, D. (2001) Effects of extrinsic imidazole ligation on molecular and electronic structure of cytochrome *c*, *J. Biol. Inorg. Chem. 6*, 628−637.
9. Banci, L., Bertini, I., Spyroulias, G. A., and Turano, P. (1998) The conformational flexibility of oxidized cytochrome *c* studied through its interaction with NH_3 and at high temperature, *Eur. J. Inorg. Chem. 1*, 583−591.
10. Shao, W., Yao, Y., Liu, G., and Tang, W. (1993) ^{1}H NMR studies of pyridine binding to cytochrome c, *Inorg. Chem. 32*, 6112−6114.
11. Shao, W., Sun, J., Yao, Y., and Tang, W. (1995) ^{1}H NMR studies of the imidazole complex of cytochrome c: Resonance assignment and structural characterization of the heme cavity, *Inorg. Chem. 34*, 680−687.
12. Liu, G., Shao, W., Huang, X., Wu, H. M., and Tang, W. (1996) Structural studies of imidazole-cytochrome c: Resonance assignments and structural comparison with cytochrome c, *Biochim. Biophys. Acta 1277*, 61−82.
13. Yao, Y., Quian, C., Ye, K., Wang, J., Bai, Z., and Tang, W. (2002) Solution structure of cyanoferricytochrome c: Ligand-controlled

conformational flexibility and electronic structure of the heme moiety, *J. Biol. Inorg. Chem. 7*, 539−547.
14. Taborsky, G., and McCollum, K. (1979) Phosphate binding by cytochrome c, *J. Biol. Chem. 254*, 7069−7075.
15. Andersson, T., Angstrom, J., Falk, K. E., and Forsen, S. (1980) Perchlorate binding to cytochrome c. A magnetic and optical study, *Eur. J. Biochem. 110*, 363−369.
16. Osheroff, N., Brautigan, D. L., and Margoliash, E. (1980) Mapping of anion binding sites on cytochrome c by differential chemical modification of lysine residues, *Proc. Natl. Acad. Sci. U.S.A. 77*, 4439−4443.
17. Craig, D. B., and Wallace, C. J. A. (1991) The specificity and K_d at physiological ionic strength of an ATP-binding site on cytochrome c suit it to a regulatory role, *Biochem. J. 279*, 781−786.
18. Barker, P. B., Bertini, I., Del Conte, R., Ferguson, S. J., Hajieva, P., Tomlinson, E. J., Turano, P., and Viezzoli, M. S. (2001) A further clue to understanding the mobility of mitochondrial yeast cytocrome c: A ^{15}N $T_{1\rho}$ investigation of the oxidized and reduced species, *Eur. J. Biochem. 268*, 4468−4476.
19. Dalvit, C., Fogliatto, G., Stewart, A., Veronesi, M., and Stockman, B. J. (2001) WaterLOGSY as a method for primary NMR screening: Practical aspects and range of applicability, *J. Biomol. NMR 21*, 349−359.
20. Sklenar, V., Piotto, M., Leppik, R., and Saudek, V. (1993) Gradient-tailored water suppression for ^{1}H-^{15}N HSQC experiments optimized to retain full sensitivity, *J. Magn. Reson., Ser. A 102*, 241−245.
21. Wider, G., Neri, D., Otting, G., and Wüthrich, K. (1989) A heteronuclear three-dimensional NMR experiment for measurements of small heteronuclear coupling constants in biological macromolecules, *J. Magn. Reson. 85*, 426−431.
22. Borgias, B., Thomas, P. D., and James, T. L. (1989) *COmplete Relaxation Matrix Analysis (CORMA)*, version 5.0, University of California, San Francisco.
23. Guntert, P., Braun, W., and Wüthrich, K. (1991) Efficient computation of three-dimensional protein structures in solution from nuclear magnetic resonance data using the program DIANA and the supporting programs CALIBA, HABAS and GLOMSA, *J. Mol. Biol. 217*, 517−530.
24. Vuister, G. W., and Bax, A. (1993) Quantitative J correlation: A new approach for measuring homonuclear three-bond $J(H^NH^\alpha)$ coupling constants in ^{15}N enriched proteins, *J. Am. Chem. Soc. 115*, 7772−7777.
25. Gagné, R. R., Tsuda, S., Li, M. X., Chandra, M., Smillie, L. B., and Sykes, B. D. (1994) Quantification of the calcium-induced secondary structural changes in the regulatory domain of troponin-C, *Protein Sci. 3*, 1961−1974.
26. Assfalg, M., Bertini, I., Turano, P., Mauk, A. G., Winkler, J. R., and Gray, B. H. (2003) ^{15}N-^{1}H residual dipolar coupling analysis of native and alkaline-K79A *S. cerevisiae* cytochrome *c*, *Biophys. J. 84*, 3917−3923.
27. Barbieri, R., Bertini, I., Cavallaro, G., Lee, Y.-M., Luchinat, C., and Rosato, A. (2002) Paramagnetically induced residual dipolar couplings for solution structure determination of lanthanide-binding proteins, *J. Am. Chem. Soc. 124*, 5581−5587.
28. Banci, L., Bertini, I., Gray, H. B., Luchinat, C., Reddig, T., Rosato, A., and Turano, P. (1997) Solution structure of oxidized horse heart cytochrome *c*, *Biochemistry 36*, 9867−9877.
29. Case, D. A., Darden, T. A., Cheatham, T. E., Simmerling, C. L., Wang, J., Duke, R. E., Luo, R., Merz, K. M., Wang, B., Pearlman, D. A., Crowley, M., Brozell, S., Tsui, V., Gohlke, H., Mongan, J., Hornak, V., Cui, G., Beroza, P., Schafmeister, C. E., Caldwell, J. W., Ross, W. S., and Kollman, P. A. (2004) *AMBER 8*, University of California, San Francisco.
30. Bertini, I., Turano, P., Vasos, P. R., Chevance, S., Bondon, A., and Simonneaux, G. (2004) Cytochrome c and SDS: A molten globule protein with altered axial ligation, *J. Mol. Biol. 336*, 489−496.
31. Garrett, D. S., Seok, Y. J., Peterkofsky, A., Clore, G. M., and Gronenborn, A. M. (1997) Identification by NMR of the binding surface for the histidine-containing phosphocarrier protein HPr on the N-terminal domain of enzyme I of the *Escherichia coli* phosphotransferase system, *Biochemistry 36*, 4393−4398.
32. Hajduk, P. J., Gerfin, T., Boehlen, J.-M., Haberli, M., Marek, D., and Fesik, S. W. (1999) High-throughput nuclear magnetic resonance-based screening, *J. Med. Chem. 42*, 2315−2317.
33. Berghuis, A. M., and Brayer, G. D. (1992) Oxidation state-dependent conformational changes in cytochrome c, *J. Mol. Biol. 223*, 959−976.
34. Baistrocchi, P., Banci, L., Bertini, I., Turano, P., Bren, K. L., and Gray, H. B. (1996) Three-dimensional solution structure of *Saccharomyces cerevisiae* reduced iso-1-cytochrome *c*, *Biochemistry 35*, 13788−13796.
35. Clore, G. M., Gronenborn, A. M., Brunger, A. T., and Karplus, M. (1985) The solution conformation of a heptadecapeptide comprising the DNA binding helix F of the cyclic AMP receptor protein of *Escherichia coli*: Combined use of ^{1}H-nuclear magnetic resonance and restrained molecular dynamics, *J. Mol. Biol. 186*, 435−455.
36. Hunter, C. A., Singh, J., and Thornton, J. M. (1991) π-π interactions: The geometry and energetics of phenylalanine-phenylalanine interactions in proteins, *J. Mol. Biol. 218*, 837−846.
37. Hobza, P., and Muller-Dethlefs, K. (2000) Noncovalent interactions: A challenge for experiment and theory, *Chem. Rev. 100*, 143−167.
38. Rashkin, M. J., and Waters, M. L. (2002) Unexpected substituent effects in offset π-π stacked interactions in water, *J. Am. Chem. Soc. 124*, 1860−1861.
39. Tsuzuki, S., Honda, K., Uchimaru, T., Mikami, M., and Tanabe, K. (2002) Origin of attraction and directionality of the π/π interaction: Model chemistry calculations of benzene dimer interaction, *J. Am. Chem. Soc. 124*, 104−112.
40. Banci, L., Bertini, I., Huber, J. G., Spyroulias, G. A., and Turano, P. (1999) Solution structure of reduced horse heart cytochrome c, *J. Biol. Inorg. Chem. 4*, 21−31.
41. Banci, L., Bertini, I., Bren, K. L., Gray, H. B., Sompornpisut, P., and Turano, P. (1997) Solution structure of oxidized *Saccharomyces cerevisiae* iso-1-cytochrome *c*, *Biochemistry 36*, 8992−9001.
42. Qi, P. X., Di Stefano, D. L., and Wand, A. J. (1994) Solution structure of horse heart ferrocytochrome c determined by high-resolution NMR and restrained simulated annealing, *Biochemistry 33*, 6408−6417.
43. Assfalg, M., Bertini, I., Dolfi, A., Turano, P., Mauk, A. G., Rosell, F. I., and Gray, H. B. (2003) Structural model for an alkaline form of ferricytochrome c, *J. Am. Chem. Soc. 125*, 2913−2922.
44. Banci, L., Bertini, I., Bren, K. L., Cremonini, M. A., Gray, H. B., Luchinat, C., and Turano, P. (1996) The use of pseudocontact shifts to refine solution structures of paramagnetic metalloproteins: Met80Ala cyano-cytochrome *c* as an example, *J. Biol. Inorg. Chem. 1*, 117−126.
45. Banci, L., Bertini, I., Bren, K. L., Gray, H. B., Sompornpisut, P., and Turano, P. (1995) Three dimensional solution structure of the cyanide adduct of *Saccharomyces cerevisiae* Met80Ala-iso-1-cytochrome c. Identification of ligand-residue interactions in the distal heme cavity, *Biochemistry 34*, 11385−11398.
46. Bren, K. L., Gray, H. B., Banci, L., Bertini, I., and Turano, P. (1995) Paramagnetic ^{1}H NMR spectroscopy of the cyanide derivative of Met80Ala-iso-1-cytochrome *c*, *J. Am. Chem. Soc. 117*, 8067−8073.
47. Banci, L., Bertini, I., Reddig, T., and Turano, P. (1998) Monitoring the conformational flexibility of cytochrome c at low ionic strength by ^{1}H NMR spectroscopy, *Eur. J. Biochem. 256*, 271−278.
48. Binkowski, T. A., Naghibzadeg, S., and Liang, J. (2003) CASTp: Computed atlas of surface topography of proteins, *Nucleic Acids Res. 31*, 3352−3355.
49. Thanos, C. D., Randal, M., and Wells, J. A. (2003) Potent small-molecule binding to a dynamic hot spot on IL-2, *J. Am. Chem. Soc. 125*, 15280−15281.
50. Thanos, C. D., Wells, J. A., and Randal, M. (2006) Hot-spot mimicry of a cytokine receptor by a small molecule, *Proc. Natl. Acad. Sci. U.S.A 103*, 15422−15427.
51. Carr, R. A., Congreve, M., Murray, C. W., and Rees, D. C. (2005) Fragment-based lead discovery: Leads by design, *Drug Discovery Today 10*, 987−992.
52. Teague, S. J., Davis, A. M., Leeson, P. D., and Oprea, T. (1999) The design of leadlike combinatorial libraries, *Angew. Chem., Int. Ed. 38*, 3743−3748.
53. Liu, X., Kim, C. N., Yang, J., Jemmerson, R., and Wang, X. (1996) Induction of apoptotic program in cell-free extracts: Requirement for dATP and cytochrome c, *Cell 86*, 147−157.
54. Banci, L., Bertini, I., Rosato, A., and Varani, G. (1999) Mitochondrial cytochromes *c*: A comparative analysis, *J. Biol. Inorg. Chem. 4*, 824−837.

BI7002857